QUANTIZED ATDHF: THEORY AND REALISTIC APPLICATIONS TO HEAVY ION FUSION

F. Grümmer
Institut für Kernphysik
Kernforschungsanlage Jülich
D-5170 Jülich, West Germany

K. Goeke
Institut für Kernphysik
Kernforschungsanlage Jülich
D-5170 Jülich, West Germany

and

Physik-Department
Universität Bonn
D-5300 Bonn, West Germany

P.-G. Reinhard[+]
Institut für Kernphysik
Universität Mainz
D-6500 Mainz, West Germany

Abstract

The quantized ATDHF theory is reviewed and discussed in the context of the generator coordinate method. This allows for a derivation which does not require an a posteriori quantization process. The ATDHF equations are then solved numerically on a coordinate and momentum grid in fully three dimensional geometry. The theory is applied to various heavy ion systems, where potentials, mass parameters and quantum corrections are evaluated and compared to conventional results from constrained Hartree-Fock. Subbarrier fusion cross sections are calculated and compared with experiment.

1. Introduction

For a couple of years adiabatic microscopic theories have been discussed as a tool to describe in a parameterfree way quantum effects of low energy and subbarrier heavy ion collisions. Actually the interest was mostly focussed on two problems, namely the quantization and the numerical evaluation of the collective path. The first one, the quantization, is to our belief basically solved, as we have emphasized already some time ago. We take here the opportunity to recall that the quantized ATDHF theory can fully be derived in the framework of the generator coordinate method (GCM) and the Gaussian overlap approximation (GOA), i.e., by means of a theory which is already quantized from the beginning. The real new thing in the present contribution is the presentation of realistic calculations of the collective path, the potentials, mass parameters and quantum corrections (zero point energies) of colliding heavy ion systems and the evaluation of fusion cross sections. This will

---

[+] Fellow of the Heisenberg-Stiftung

actually demonstrate that quantized ATDHF together with the corresponding validity condition is indeed a solvable theory which allows, e.g., the use of present time well established density dependent forces and coordinate space techniques. The paper is constructed in the following way: Section 2 recalls the Gaussian overlap approximation in the GCM and review the derivation of quantized ATDHF by means of GCM. Section 3 explains the way how the optimal collective path is obtained numerically and shows some results regarding the masses and potentials of the systems $\alpha+\alpha \Leftrightarrow {}^{8}Be$, ${}^{12}C+{}^{12}C \Leftrightarrow {}^{24}Mg$, and ${}^{16}O+{}^{16}O \Leftrightarrow {}^{32}S$. Here also the constrained HF method, yielding a different collective path, is discussed. Section 4 shows the application to subbarrier fusion cross sections; some conclusions and an outlook are given in section 5.

2. The Derivation of Quantized ATDHF from GCM

Quantized ATDHF is a consistent microscopic theory for large amplitude collective motion. It provides first an equation determining an optimal collective path, second a unique quantized collective Hamiltonian (for the motion within that collective basis), third a simple prescription for evaluating any desired expectation value and transition moment within the collective states, and fourth it allows to check a posteriori the validity of the collective description. The theory has been derived in three independent ways. We will give here a short account of the derivation from the generator coordinate method (GCM) which is the most satisfying for its conceptual clarity.

We start out from the concept of a collective path $\{|\Phi_q\rangle\}$, which is a set of collectively deformed Slater determinants (or BCS states), where q labels somehow the deformation. This set $\{|\Phi_q\rangle\}$ is supposed to be an expansion basis along which the actual collective motion does evolve. This means quantum mechanically that we consider the superposition

$$|\psi\rangle = \int dq \; |\Phi_q\rangle \, f(q) \tag{2.1}$$

where the actual collective dynamics is described by f(q). As a means to optimize the collective superposition f(q) as well as the basis $\{|\Phi_q\rangle\}$ we are going to use the stationary variational principle

$$\langle\delta\psi|\hat{H}-E|\psi\rangle = 0 \tag{2.2}$$

In this general form, however, the equations turn out to be impractical, since complicated kernels $\langle\Phi_q|H|\Phi_{q'}\rangle$ arise, and, even worse, they are not specific enough for a variation $\langle\delta\Phi_q|$ since the ansatz (2.1) still embraces the full Hilbert space if no further assumption for the basis $\{|\Phi_q\rangle\}$ is made.

An obvious requirement for a tractable $|\Phi_q>$ is that it is analytical in q. Furthermore, the $\{|\Phi_q>\}$ ought to represent a series of collective deformations, where a small displacement of many particles adds up coherently to a substantial reordering of the matter. Hence the overlaps $<\Phi_q|\hat{O}_p|\Phi_{q'}>$ should be continuous and fall off rapidly with rising (q-q'). Therefore, it is reasonable to assume Gaussian overlap for the norm kernel

$$<\Phi_q|\Phi_{q'}> = \exp\left(-\frac{\lambda(\frac{q+q'}{2})}{4}(q-q')^2\right) \tag{2.3}$$

where $\lambda = 2<\Phi_q|\overleftarrow{\partial}_q\overrightarrow{\partial}_q|\Phi_q>$ and a Gaussian times a polynomial in (q-q') for the overlap $<\Phi_q|\hat{O}|\Phi_{q'}>$ of any operator O different from unity.

Working out this Gaussian overlap approximation (GOA) we obtain for any operator $\hat{O}$ the expectation value[1)]

$$<\psi|\hat{O}|\psi>_{GOA} = \int dq\ g^*(q)\ \{(1 - \frac{1}{4\lambda}\partial_q^2)<\Phi_q|\hat{O}|\Phi_q>$$

$$- : \frac{d}{dq}, <\Phi_q|\overleftarrow{\partial}_q\bar{O} - \bar{O}\overrightarrow{\partial}_q|\Phi_q> : + \frac{1}{2} : (\frac{d^2}{dq^2} + \frac{\lambda}{2}), <\Phi_q|\overleftarrow{\partial}_q^2\bar{O} - 2\overleftarrow{\partial}_q\bar{O}\partial_q + \hat{O}\overrightarrow{\partial}_q^2|\Phi_q>: \}g(q) \tag{2.4}$$

where ∂_q acts only on an $|\Phi_q>$ or $<\Phi_q|$ while $\frac{d}{dq}$ is acting on everything at the right. The :...: is the normal ordering, $: (\frac{d}{dq})^n + \lambda, A(q) : = 2^{-n}\{\frac{d}{dq}, \ldots, \{\frac{d}{dq}, A\}\ldots\} + \lambda A$. The g(q) is the collective wave function, related to the superposition f(q) by ref. 1)

$$g(q) = \int dq'\ (\lambda/\pi)^{1/4} \exp\left(-\frac{\lambda}{2}(q-q')^2\right) f(q') \tag{2.5}$$

as follows from the GOA.

If g(q) is normalized as $\int dq\ g^*(q)g(q) = 1$, the $|\psi>$ is normalized to unity, $<\psi|\psi> = 1$. The $\bar{O}$ is a shorthand for $\bar{O} = \hat{O} - <\Phi_q|\hat{O}|\Phi_q>$. The eq. (2.4) is the key formula for all further developments. It can easily be generalized to the case of a many parameter GCM.

The GCM-GOA now is a useful starting point for all further developments. In particular, it allows to apply the variational principle

$$<\delta\psi|H-E|\psi>_{GOA} = 0 \tag{2.2b}$$

for both variations, $<\delta\Phi_q|$ and δg^*, leading eventually to unambiguous results and workable equations. To derive the quantized ATDHF we make some further assumptions about the collective basis. In order to avoid the well known shortcoming of GCM to yield for Slater determinants $|\Phi_q>$ in case of pure translation not the proper

collective mass resulting from Galilei invariance, we are using a dynamic basis $\{|\Phi_{qp}>\}$ where p labels the momentum conjugate to q (this is a generalization of the Thouless-Peierls double projection method). Such a dynamic basis, however, is hard to treat in general. We therefore consider only the adiabatic expansion of it

$$|\Phi_{qp}> = |\Phi_q> + i\, p\, Q(q)|\Phi_q> \tag{2.6}$$

In that small-p expansion the p-dynamics can be solved[1] explicitly by means of GOA and RPA techniques, leading to an RPA correlated basis $\{|\tilde{\Phi}_q>\}$ where the dynamic information up to order p^1 is built in by the redundancy property

$$\lambda\, \hat{Q}(q)|\tilde{\Phi}_q> = \partial_q|\tilde{\Phi}_q> \tag{2.7}$$

For the new basis we obtain[1] any expectation value as

$$<\psi|\hat{O}|\psi>_{GOA} = \int dq\, \tilde{g}^*(q)\{(1 - \frac{1}{4\lambda}\partial_q^2|<\tilde{\Phi}_q|\hat{O}|\tilde{\Phi}_q> + :\frac{d}{dq}<\tilde{\Phi}_q|[\bar{O},\hat{Q}(q)]|\tilde{\Phi}_q>:$$
$$+\frac{1}{2}:|-\frac{d^2}{dq^2} - \frac{\lambda}{2}|<\tilde{\Phi}_q|[\hat{Q}(q),[\hat{O},\hat{Q}(q)]]|\tilde{\Phi}_q>:\}\tilde{g}(q) \tag{2.8}$$

Now we apply the path variation $<\delta\tilde{\Phi}_q|$ for the case $\hat{O} = \hat{H}-E$ requiring in addition independency, which means that the set $\{|\Phi_q>\}$ should be a basis for a whole collective spectrum and therefore be independent of the actual collective state g(q). This yields[2] the ATDHF equations for the states $|\Phi_q>$, which are in this GCM context the single particle vacua associated to the correlated states $|\tilde{\Phi}(q)>$. The $\{|\Phi_q>\}$ set up the collective path and obey the well known ATDHF equations[3,4].

$$<\Phi_q|a^+a(\hat{H}-\partial_q V\hat{Q})|\Phi_q> = 0 \tag{2.9a}$$

$$<\Phi_q|a^+a([H,\hat{Q}] - \frac{1}{M}\overrightarrow{\partial}_q)|\Phi_q> = 0 \tag{2.9b}$$

where V is the collective potential

$$V(q) = <\Phi_q|\hat{H}|\Phi_q> \tag{2.9c}$$

M is the collective mass

$$M^{-1}(q) = <\Phi_q|[\hat{Q}(q),[\hat{H},\hat{Q}(q)]]|\Phi_q> \tag{2.9d}$$

and $\hat{Q}$ is normalized according to

$$<\Phi_q|\hat{Q}(q)\overrightarrow{\partial}_q + \overleftarrow{\partial}_q\hat{Q}(q)|\Phi_q> = -1 \tag{2.9e}$$

This is a coupled set of equations determining at once the path $|\Phi_q>$, the $\hat{Q}(q)$, the mass $M(q)$ and the potential $V(q)$.

Using $\hat{O} = \hat{H}-E$, the variation of eq. (2.8) with respect to $\delta g^*(q)$ yields immediately the quantized collective Hamiltonian[1,2]

$$(\hat{H}_{coll}-E)g(q) = 0 \tag{2.10a}$$

with

$$\hat{H}_{coll} = -\frac{1}{8}\left\{\frac{d^2}{dq^2}\frac{1}{M} + 2\,\frac{d}{dq}\frac{1}{M}\frac{d}{dq} + \frac{1}{M}\frac{d^2}{dq^2}\right\} + V(q) - Z(q) \tag{2.10b}$$

where $Z(q)$ includes the quantum corrections (zero-point energies) contained in the states $|\Phi_q>$,

$$Z(q) = \frac{\lambda}{4M} + \frac{1}{4\lambda}\,\partial_q^2 V + Z_{rot} + Z_{trans} \tag{2.10c}$$

Apparently in the present derivation the quantization is already naturally built in and no further a posteriori step is necessary.

In practice, we will consider always more than one collective coordinate, at least the two rotational angles ϑ,φ together with the axial deformation q. Therefore the $Z(q)$ contains the corresponding rotational zero-point energy Z_{rot} and, because of spurious center-of-mass motion, also a corresponding Z_{trans}. Actually, in eq. (2.10) the correlated $|\tilde{\Phi}_q>$ do not appear explicitly but only the Slater determinants $|\Phi_q>$. The big difference to an ordinary GCM starting directly from $|\Phi_q>$ rather than from $|\tilde{\Phi}_q>$ or $|\Phi_{qp}>$ lies in the expression for the mass parameter M in eqs. (2.10b), (2.10c). This mass is now the asymptotically correct mass being of Peierls-Thouless rather than of Peierls-Yoccoz form. It is the well known ATDHF mass obtained by GCM. The other corrections, originating from a GCM over $\tilde{\Phi}_q$ rather than Φ_q are negligible. For details of this procedure see ref. 1).

If we have determined the basis according to the ATDHF equations (2.9) and solved the collective Schrödinger equation (2.10), we can evaluate any desired expectation value according to eq. (2.8). In other words, eq. (2.8) provides us with a translation of any operator $\hat{O}$ into collective space

$$\tilde{\hat{O}}_{coll} = (1 - \frac{1}{4\lambda}\,\partial_q^2)<\Phi_q|\hat{O}|\Phi_q> + :\frac{d}{dq}<\Phi_q|\bar{[\hat{O},\hat{Q}(q)]}|\Phi_q>:$$
$$-\frac{1}{2}:\left[\frac{d^2}{dq^2}+\frac{\lambda}{2}\right],<\Phi_q|\bar{[\hat{Q}(q),[\hat{O},\hat{Q}(q)]]}|\Phi_q>: \tag{2.11a}$$

and any transition moment is easily evaluated as a simple q-integration

$$\langle\psi_f|\hat{O}|\psi_i\rangle_{GOA} = \int dq\; g_f^*(q)\; \hat{O}_{coll}\; g_i(q) \tag{2.11b}$$

Finally we can derive a criterion for the validity of the collective description thus obtained[5,6]. To this end one evaluates perturbationally the coupling of the space $\{|\Phi_q\rangle\}$ to the 1p-1h neighbourhood $\{|\Phi_q\rangle, a_p^+ a_h|\Phi_q\rangle\}$. This eventually leads to the so-called "validity condition"

$$(\frac{p^2}{2})^2\; \langle\Phi_q|\tilde{X}_\perp^2|\Phi_q\rangle << 1 \tag{2.12a}$$

where X is the solution of

$$[H,\hat{X}]_{ph} = -i\;[[H,\hat{O}],Q]_{ph} - \frac{i}{M}\,(\partial_q Q)_{ph} \tag{2.12b}$$

and

$$\hat{X}_\perp = \hat{X} - \hat{Q}\,\langle\Phi_q|\overleftarrow{\partial}_q\hat{X} + \hat{X}\overrightarrow{\partial}_q|\Phi_q\rangle \tag{2.12c}$$

Thus altogether we have set up a consistent theory which yields eqs. (2.9) for an optimal collective basis, eqs. (2.10) for a quantized collective Hamiltonian, eqs. (2.11) for evaluating transition moments and expectation values, and finally eqs. (2.12) for an a posteriori check.

3. Numerical Solution of the ATDHF Equations

The first and indeed most difficult step consists in solving the ATDHF eqs. (2.9) in order to obtain the optimal collective path $\{|\Phi_q\rangle\}$. The only way, which has led to numerical results in realistic cases, has been suggested in ref. 7). It consists in transforming[7] eqs. (2.8) to one single differential equation for $\{|\Phi_q\rangle\}$

$$\frac{\partial}{\partial q}|\Phi_q\rangle = \bar{\varepsilon}(q)\;[H,H_{ph}]_{ph}|\Phi_q\rangle \tag{3.1}$$

with

$$\bar{\varepsilon}(q) = M(q)\,(\frac{\partial V}{\partial q})^{-1} \tag{3.2}$$

Apparently eq. (3.1), being equivalent to the ATDHF eqs. (2.9), is an initial value problem: For any choice of an initial value $|\Phi_{q_0}\rangle$ one obtains a collective path $\{|\Phi_q^{(q_0)}\rangle\}$, which shows that the old formulations of ATDHF[3] were not unique. An illustration of several solutions is given in fig. 1, where some resulting trajectories of eq. (3.1) are evaluated in a two dimensional landscape model[8]. One realizes that all solutions converge towards the special solution of eq. (3.1) extending from the saddle point towards the HF minimum. As has been shown in ref. 9)

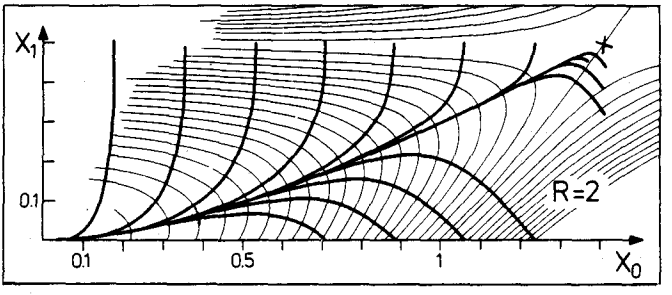

ATDHF - theory: Goeke - Reinhard

Figure 1

these solutions are, in differential geometrical terms, "fall lines with respect to the mass tensor" and the fall line from the saddle to the HF minimum is the fall line closest to a geodesic between these points. It is very important, and shows the relevance of the validity condition, that the fall line from saddle to HF can be shown[8] to fulfil best the validity condition. Hence it is the desired optimal collective path. It should be remarked that the ATDHF equations need the complement[7] of the validity condition[5,6] to yield this unique result. Thus for the numerical procedure one has first to find the saddle point and then one can solve eq. (3.1).

The eq. (3.1) is solved by means of the Euler-Step-Method. There one solves eq. (3.1) in successive steps n = 0,1,2,... with

$$|\Phi^{(n+1)}> = \{1 - \varepsilon\, [H,H_{ph}]_{ph}\}|\Phi^{(n)}> \qquad (3.3)$$

Here the point n=0 is close to the saddle point and $\varepsilon = 10^{-4}$ MeV^{-2} is a small stabilizing constant. In the present calculations eq. (3.3) is solved using the Bonche-Koonin-Negele force[10] completed by a direct Coulomb potential. The evaluation is done in the coordinate space using a three dimensional grid of dimensions 24x16x16 with a meshsize of 1 fm. For the evaluation of the kinetic energy the wave functions are Fourier-transformed and smoothed by restricting the Fourier components to $k \leq k_{max}$ with $(\hbar k_{max})^2/2m \leq 130$ MeV. This also simplifies the storage in the computer. The wave functions are furthermore simplified by assuming quartet symmetry (averaged Coulomb) and good parity of the single particle wave functions with respect to reflections at the x-y-, y-z- and x-z-planes.

Fig. 2 shows for the α-α system the energies $<\Phi_n|H|\Phi_n>$ associated to various $|\Phi^{(n)}>$ where different initial starting points were chosen. One sees immediately how the saddle point is identified and how the various trajectories converge towards the optimal path, i.e., the one from saddle point towards HF or towards fragmentation. The wave functions $|\Phi^{(n)}>$ are labelled with the distance R of the ions extracted from the total quadrupole moment by means of

$$\frac{1}{2} A R^2 = <\Phi|r^2 Y_2|\Phi> - Q_1 - Q_2$$

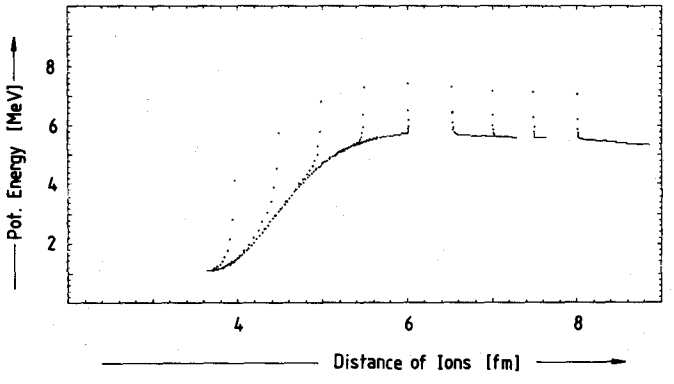

Figure 2

where A is the total nucleon number and Q_1 and Q_2 are the quadrupole moments of the initial fragments. This labelling is convenient and allows an immediate interpretation of the collective wave function in the asymptotic region of separate fragments. However in principle any other labelling could be used since the physical properties of the system as e.g. energies, transition moments, penetration coefficients, etc. are independent of the label.

The final results of the $\alpha+\alpha \leftrightarrow {}^{8}Be$ system are given in fig. 3, where the classical potential V(R), the quantum corrected V(R)-Z(R) (see eq. (2.10)), and the collective mass M(R) associated to the relative motion are given. One notices that the M(R) approaches the correct asymptotic value of $\mu = 2$ m for large separation distances of the ions. The M(R) is by no means constant but shows a clear bump at R = 4.7 fm with a value of M(R) = 2.8 m. This bump indicates at which distance the internal rearrangements on the way from the separated system to the compound nucleus take place. The fig. 4 shows the zero-point energies for the various degrees of freedom and the total zero-point energy. Apparently the Z(R) reaches a value of about 2 MeV and is therefore not at all negligible, as it is often assumed in the literature.

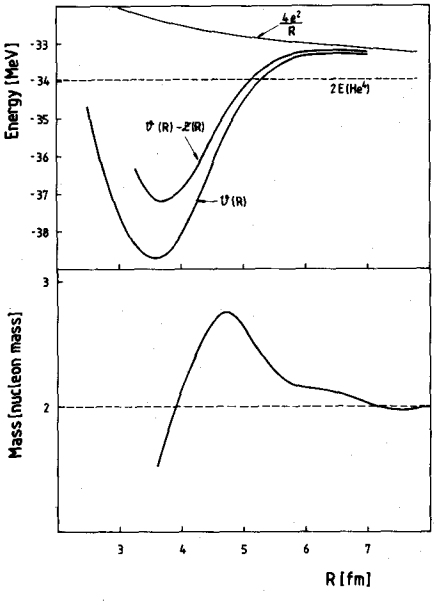

Figure 3

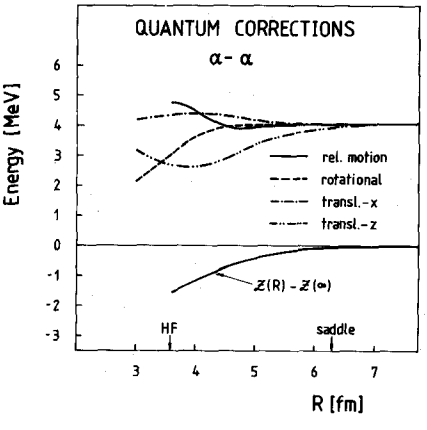

Figure 4

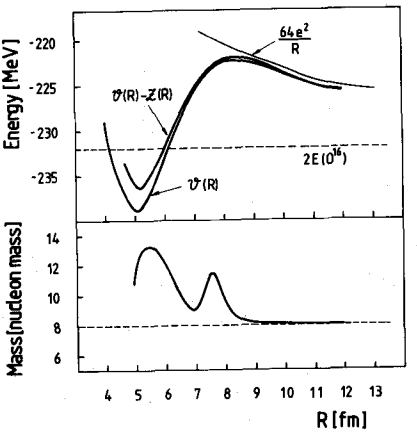

Figure 5

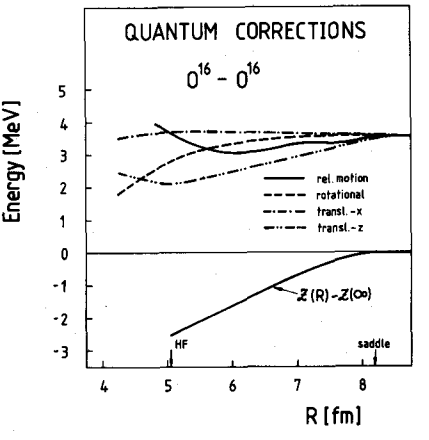

Figure 6

The collective potentials and the mass parameter for the $^{16}O+^{16}O \leftrightarrow {}^{32}S$ fusion reaction are given in fig. 5 and the zero-point energies of this process in fig. 6. Here the mass parameter shows two bumps, one close to the HF-point and one half-way to the saddle point. The fact that the potentials rise few distances smaller than the HF-point at R = 5 fm is due to the reflection symmetries used and due to the lack of pairing correlations. The potential V(R)-Z(R) should lie below the classical potential V(R), however the V(R) is shifted such that it exhibits the pure Coulomb tail as V(R)-Z(R) does. Similar curves for the $^{12}C+^{12}C \leftrightarrow {}^{24}Mg$ system are given in figs. 7 and 8. There one has to distinguish between an axial and a triaxial configuration depending on whether the two oblate ^{12}C nuclei are parallel to each

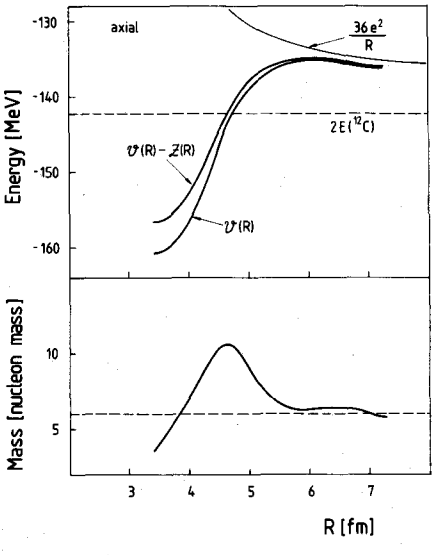

Figure 7

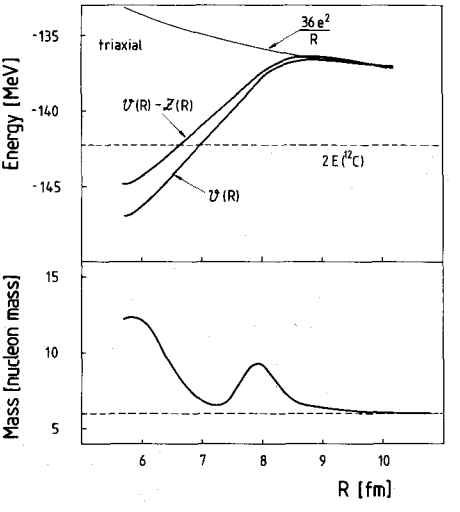

Figure 8

other or whether they are lying in a plane. Apparently the corresponding potentials and masses are quite different. The saddle point for the triaxial configuration, e.g., lies at a distance which is 3 fm larger than for the axial configuration. In addition the masses show different peaks.

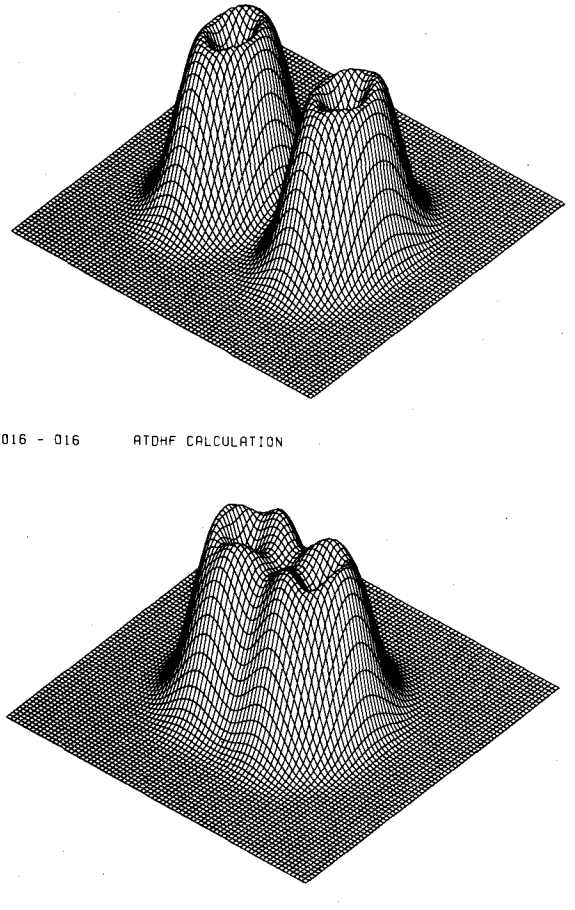

Figure 9

The fig. 9 shows density distributions for the $^{16}O+^{16}O \leftrightarrow {}^{32}S$ system at two relevant R-values close to the saddle point and close to the HF-point of the $^{16}O+^{16}O$ system, respectively. The central depression in the ^{16}O fragments is due to the BKN-interaction used which lacks the ls-term. One realizes that the neck degrees of freedom are fully incorporated. Fig. 10 shows a cut through the density distributions along the axis connecting the fragments, which is chosen to be the z-axis. One realizes even for an adiabatic reaction a small density pile up in the central region at R = 6.6 fm compared to the relaxed HF-state at R = 5.0 fm. Figs. 11 and 12 show contour plots of the density of the $^{12}C+^{12}C \leftrightarrow {}^{24}Mg$ system.

It is interesting to compare the collective path obtained by the present ATDHF method with the one obtained by conventional constrained Hartree-Fock techniques. The standard choice for the constraint in the present systems is the quadrupole operator. Flocard et al.[11,12] have done calculations for the $^{16}O+^{16}O \leftrightarrow {}^{32}S$, $^{12}C+^{12}C \leftrightarrow {}^{24}Mg$ and recently for the $^{40}Ca+^{40}Ca \leftrightarrow {}^{80}Zr$ system. Besides the method used the technicalities of these calculations were similar to the ones used here. Thus the results are directly comparable. Whereas the potentials are not much different the mass parameters turn

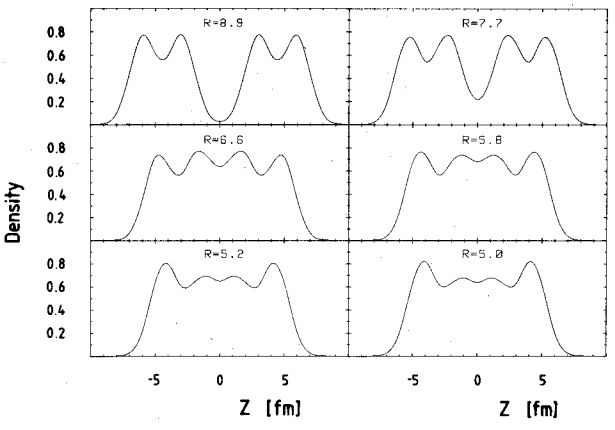

Figure 10

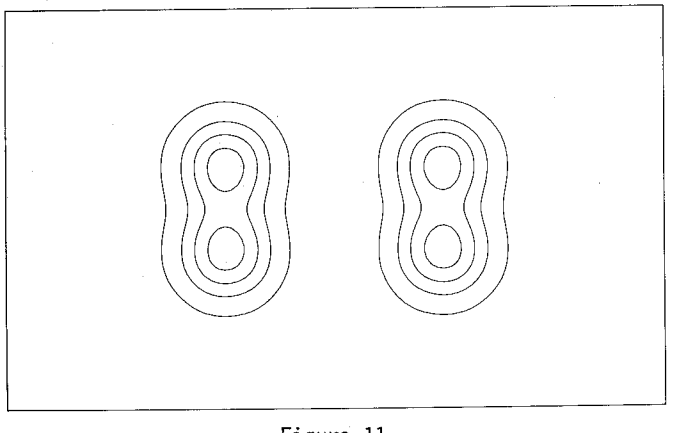

Figure 11

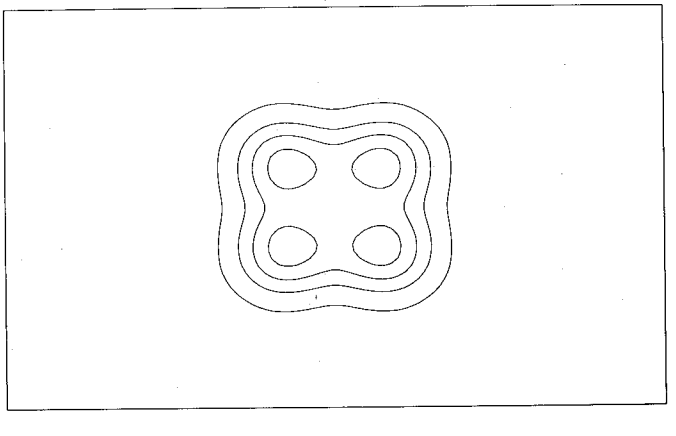

Figure 12

out to be very sensitive to the path used, CHF or ATDHF. This can be seen at fig. 13 which can be directly compared to Heenen's fig. 1 in these proceedings. Apparently the masses are totally different, showing strange peaks in the CHF case. This actually demonstrates that CHF is a rather poor approximation to ATDHF. Indeed the constraining operator $\hat{Q}$ of eq. (2.9a) is allowed to be nonlocal and R-dependent in contrast to the constraint r^2Y_{20} as used in CHF. That indeed $\hat{Q}$ is highly nonlocal has long time ago been demonstrated in ref. 13) for the monopole vibration of ^{16}O using the Skyrme-3 interaction. In fig. 14, not given in ref. 13), the quantity $\chi(r,r')/\dot{q}$ is plotted which is proportional to $Q(r,r')$ in this example. The case $^{16}O+^{16}O \leftrightarrow ^{32}S$ is by no means an exception. Figs. 15 and 16 show similar comparisons for the $\alpha+\alpha \leftrightarrow ^{8}Be$ and $^{12}C+^{12}C \leftrightarrow ^{24}Mg$ systems.

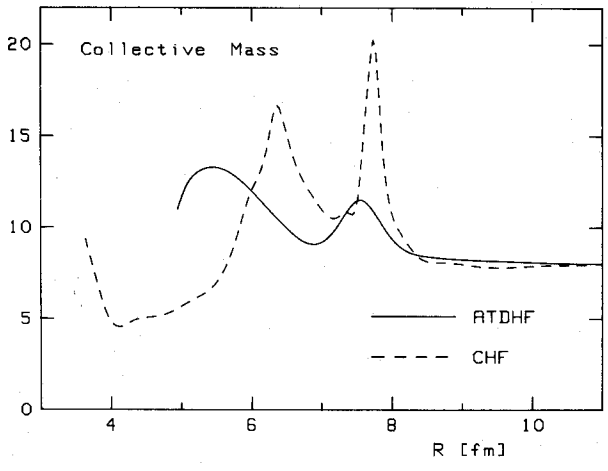

Figure 13

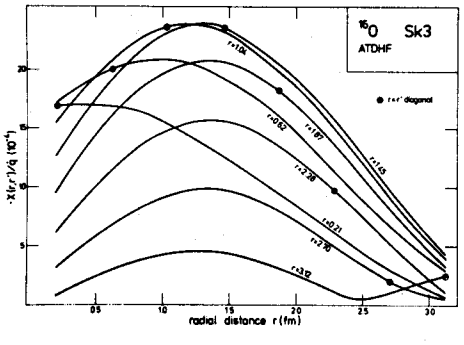

Figure 14

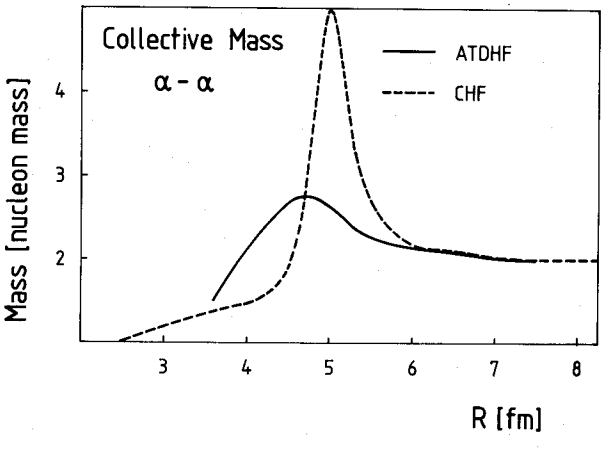

Figure 15

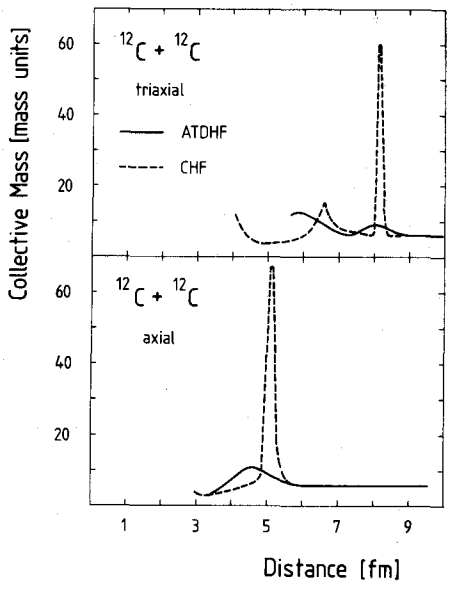

Figure 16

4. Application of Quantized ATDHF to Nuclear Fusion

Except the mass parameter M(R), being asymptotically correct, the classical potential V(R) and the quantum corrections Z(R), we also have calculated the rotational moment of inertia of the total system, $\Theta(R)$, in the GCM or Peierls-Yoccoz approximation. This allows one to complete the collective Hamiltonian of eq. (2.10) by a centrifugal term $L(L+1)/2\Theta(R)$ in order to evaluate also higher partial waves. If one inserts all these quantities into the eq. (2.10) one can easily evaluate transmission coefficients corresponding to the penetration through the barrier by using WKB-techniques:

$$T_L(E_{CM}) = \exp\{-2\, I_L(E_{CM})\} \tag{4.1}$$

with

$$I_L(E_{CM}) = \int_a^b \{\frac{2M(R)}{\hbar^2}(V(R)-Z(R) + \frac{\hbar^2}{2\Theta(R)} L(L+1) - E_{CM})\}dR \tag{4.2}$$

where a and b are the classical turning points. From these quantities one can easily evaluate the fusion cross section for identical fragments:

$$\sigma_{fus}(E_{CM}) = \frac{2}{k^2} \sum_{L=\text{even}} (2L+1)T_L(E_{CM}) \tag{4.3}$$

For the $^{16}O+^{16}O \leftrightarrow {}^{32}S$ fusion the cross section of quantized ATDHF in comparison with the experimental values is given in fig. 17. One realizes that one can evaluate σ_{fus} even at very low energies where the experimental counting rate is too low to allow for reliable measurements. This is perhaps relevant for the description of thermonuclear burning in stellar systems which, if one includes the Gamow-peak, requires cross sections at a few MeV. A more detailed comparison with experimental data can be done if one considers instead of the fusion cross section the astrophysical S-factor defined as

$$\sigma_{fus}(E_{CM}) = \frac{1}{E_{CM}} S(E_{CM}) \exp\{-\frac{2\pi Z_1 Z_2 e^2}{\hbar v}\}$$

with v being the relative velocity. The S-factor for quantized ATDHF is given in fig. 18 in comparison to the experimental data and the values extracted from CHF.

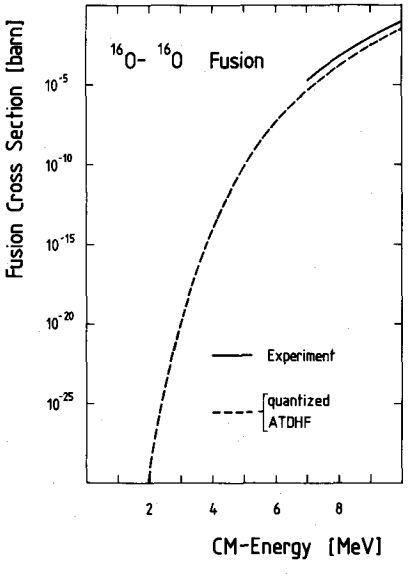

Figure 17

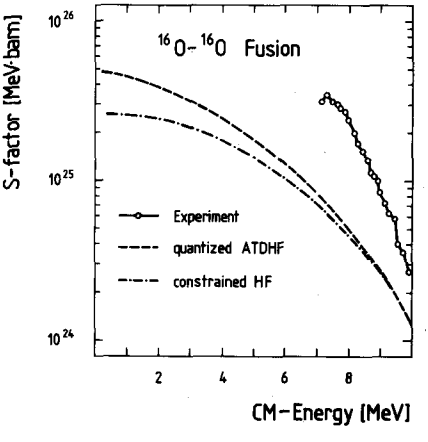

Figure 18

Although quantized ATDHF is closer to experiment than CHF still a factor 2-5 is missing and the trend versus E_{CM} is poorly reproduced. The reason for this is still to be found out. Such an investigation certainly has to incorporate a detailed study of the TDHF fusion cross sections slightly above the barrier. It is very probable that the lack of the ls-component of the nuclear interaction has a strong impact on the subbarrier results, perhaps more than on superbarrier properties.

5. Conclusion

The present article shows that quantized ATDHF is indeed a theory which besides conceptual merits allows also for clean numerical solutions.

Quantized ATDHF provides a variational way to extract the optimal collective path from which a fully quantized collective Hamiltonian with one dynamical collective coordinate can be extracted. The resulting collective wave functions allow one a clear interpretation in terms of matrix elements of observables. All quantities necessary can be and have been evaluated using techniques in a three dimensional coordinate and momentum grid (lattice) similar to techniques known from TDHF calculations. In contrast to TDHF the domain of applications of quantized ATDHF are typical quantum properties as e.g. subbarrier fusion cross sections, examples to which are given in this article, where the light ion systems $\alpha+\alpha \leftrightarrow {}^{8}Be$, ${}^{12}C+{}^{12}C \leftrightarrow {}^{24}Mg$ and ${}^{16}O+{}^{16}O \leftrightarrow {}^{32}S$ are considered. More detailed studies concerning a greater variety of nuclear systems, better interactions, less restrictive symmetries and the inclusion of pairing correlations are required and will be the task for the near future.

References

1) K. Goeke, P.-G. Reinhard, Ann. Phys. 124 (1980) 249.
2) P.-G. Reinhard, K. Goeke, Phys. Rev. C20 (1979) 1546.
3) F. Villars, Nucl. Phys. A285 (1977) 269.
4) K. Goeke, P.-G. Reinhard, Ann. Phys. 112 (1978) 328.
5) P.-G. Reinhard, K. Goeke, Phys. Lett. 69B (1977) 17.
6) P.-G. Reinhard, K. Goeke, Nucl. Phys. A312 (1978) 121.
7) P.-G. Reinhard, J.A. Maruhn, K. Goeke, Phys. Rev. Lett. 44 (1980) 1740.
8) K. Goeke, P.-G. Reinhard, D.J. Rowe, Nucl. Phys. A359 (1981) 408.
9) D.J. Rowe, A. Ryman, J. Math. Phys. 23 (1982) 732.
10) P. Bonche, S. Koonin, J. Negele, Phys. Rev. C13 (1976) 1226.
11) H. Flocard, P.H. Heenen, D. Vautherin, Nucl. Phys. A339 (1980) 336.
12) P.H. Heenen, H. Flocard, D. Vautherin, these proceedings.
13) K. Goeke, Phys. Rev. Lett. 38 (1977) 212.